

ARTICLE

Influence of Triarylamine and Indoline as Donor on Photovoltaic Performance of Dye-Sensitized Solar Cells Employing Cobalt Redox Shuttle

Yue Zhang^a, Zhi-hui Wang^b, Yu-jie Hao^b, Quan-ping Wu^a, Mao Liang^b, Song Xue^{b*}

a. Tianjin Key Laboratory of Control Theory & Applications in Complicated Systems, Tianjin University of Technology, Tianjin 300384, China

b. School of Chemistry & Chemical Engineering, Tianjin University of Technology, Tianjin 300384, China

(Dated: Received on September 16, 2014; Accepted on January 21, 2015)

Two organic dyes **XS51** and **XS52** derived from triarylamine and indoline are synthesized for dye-sensitized solar cells (DSCs) employing cobalt and iodine redox shuttles. The effects of dye structure upon the photophysical, electro-chemical characteristics and cell performance are investigated. **XS51** with four hexyloxy groups on triarylamine performs better steric hindrance and an improvement of photovoltage. **XS52** provides higher short-circuit photocurrent density due to the strong electron-donating capability of indoline unit. The results from the redox electrolyte on cell performances indicate that the synthesized dyes are more suitable for tris(1,10-phenanthroline)cobalt(II/III) redox couple than I^-/I_3^- redox couple in assembling DSCs. Application of **XS52** in the cobalt electrolyte yields a DSC with an overall power conversion efficiency of 6.58% under AM 1.5 (100 mW/cm²) irradiation.

Key words: Dye-sensitized solar cells, Indoline, Triarylamine, Photovoltaic, Cobalt redox shuttle

I. INTRODUCTION

Dye-sensitized solar cells (DSCs), as a new type of photovoltaic technology, have been considered to be a credible alternative to conventional inorganic silicon-based solar cells because of their ease of fabrication, high efficiency, and cost-effectiveness [1, 2]. During the last two decades, many different photosensitizers, including metal complexes, porphyrins, phthalocyanines and metal-free organic dyes, have been designed and applied into DSCs [2]. Among them, triarylamine organic dye-sensitized solar cells employing widely used iodine (I^-/I_3^-) electrolytes have reached power conversion efficiencies as high as 10%–11% [3], comparable to those of Ru complexes. Nevertheless, iodine redox couple also shows some drawbacks, which limit further improvement of DSCs' performance, such as the relatively high overpotential that has led to a noticeable energy loss [4], the larger charge recombination rate at the titania/electrolyte interface [5–7], the light harvesting loss [8, 9], and the corrosiveness of I^-/I_3^- redox couple [10, 11]. To achieve a breakthrough in developing highly efficient DSCs, alternative redox couples, including metal complexes, hole conductors, halogens and pseudo-

halogens and some redox active organic compounds [12] have been explored for DSCs to avoid the above problems. During the past few years, researchers have made astonishing progress by moving from a multi-electron iodide/tri-iodide redox couple to one-electron outer-sphere redox couples, such as cobalt complexes [1, 13–15]. A combination of zinc porphyrin dye (YD2-o-C8) and organic dye (Y123) showed an excellent efficiency of 12.3% employing tris(2,2'-bipyridine)cobalt(II/III) redox couple [1]. The cobalt(II/III) complex with a tridentate ligand 6-(1H-pyrazol-1-yl)-2,2'-bipyridine (bpy-pz) yielded a power conversion efficiency of over 10% at 100 mW/cm² in combination with Y123 [16]. Wang *et al.* explored tris(1,10-phenanthroline)cobalt(II/III) redox shuttles in conjunction with the triphenylamine-based organic dyes, displaying power conversion efficiency of 9.4% [17]. A remarkable advantage of cobalt redox shuttle over I^-/I_3^- redox couple is that very high open-circuit voltage (V_{oc}) can be achieved without reducing short circuit photocurrent or fill factor [3, 10]. However, the slow mass transport of cobalt redox shuttle and increased recombination of injected electrons with the oxidized redox species in the electrolyte may lead to poorly performing devices with low photovoltages and photocurrents [9, 18–20]. To overcome the disadvantages of cobalt redox shuttle, a relatively thin TiO₂ film and high extinction coefficient photosensitizers with steric properties are warranted for high efficiency of the dye-sensitized solar cells.

* Author to whom correspondence should be addressed. E-mail: xuesong@ustc.edu.cn

Recently, we have demonstrated that functionalized-indoline-based organic dyes possess high extinction coefficients apart from their impressive short-circuit photocurrent density (J_{sc}), benefit from the powerful electron-donating capability of the indoline unit [21]. The bulky rigid groups (*i.e.* dipropylfluorene and hexapropyltruxene unit) on the dyes retard electron transfer from the conduction band of TiO_2 to the oxidized redox species in the electrolyte, which enables the attainment of high photovoltages. As a part of our systematic development of bulky organic dyes, we have designed and synthesized an organic dye with hexyloxy group on indoline moiety. The long alky chains on the dye prefer to perform good steric hindrance for improvement of photovoltage. The alkoxy substituents on indoline moiety are expected to further enhance the electron-donating capability of dye donor for attainment of high J_{sc} . The classical 3,4-ethylenedioxythiophene (EDOT) is used as π -conjugated spacer for its broadening absorption spectra and good light harvest. For comparison, a triarylamine dye with the similar hexyloxy group and conjugated bridging segment (π) is synthesized for understanding the relationship of dye structure and cell performance. Their molecular structures are shown in Fig.1.

II. MATERIAL AND METHODS

A. General synthetic procedure

The synthetic route for **XS51** and **XS52** is shown in Scheme 1 and 2. All the reactions were conducted under nitrogen atmosphere in oven dried glassware with magnetic stirring. Diethyl ether and THF were dried and distilled from sodium and benzophenone under nitrogen protection. Phosphorus oxychloride was freshly distilled before use. Dichloromethane was dried and freshly distilled from calcium hydride under nitrogen atmosphere. All other solvents and chemicals used in this work were analytical grade without further purification. Melting points of the samples were taken on an RY-1 melting point apparatus (Tianfen, China). 1H NMR and ^{13}C NMR spectra were recorded on Bruker 400 instruments by using the residual signals $\delta=7.26$ and 77.0 ppm from $CDCl_3$, $\delta=2.50$ and 39.4 ppm from $DMSO-d_6$. High resolution mass spectra were obtained with a Micromass GIQ-TOF mass spectrometer.

B. Detailed experimental procedures and characterization

1. Preparation of compound 3

Tris(4-bromophenyl)amine **1** (1.16 g, 2.4 mmol), 2-(2,5-bis(hexyloxy)phenyl)-4,4,5,5-tetramethyl-1,3,2-dioxaborlone **2** (1.94 g, 4.8 mmol), K_2CO_3 (827.5 mg,

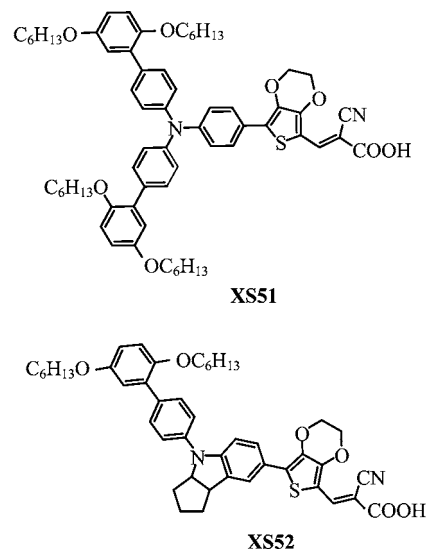
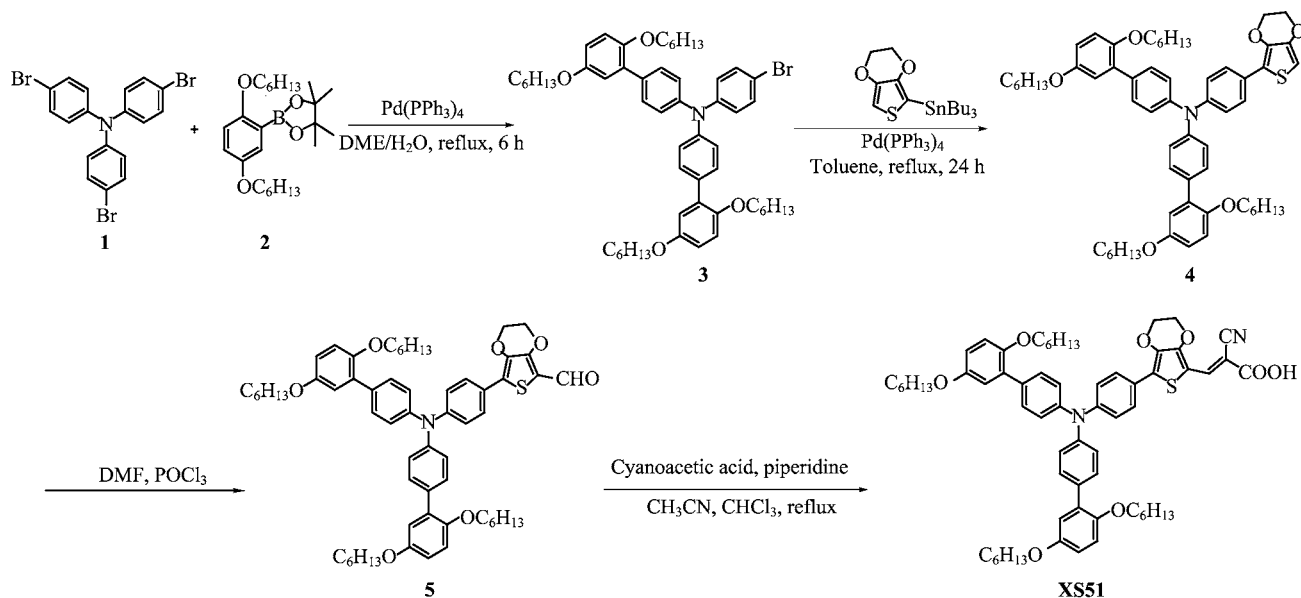


FIG. 1 Chemical structures of **XS51** and **XS52**.

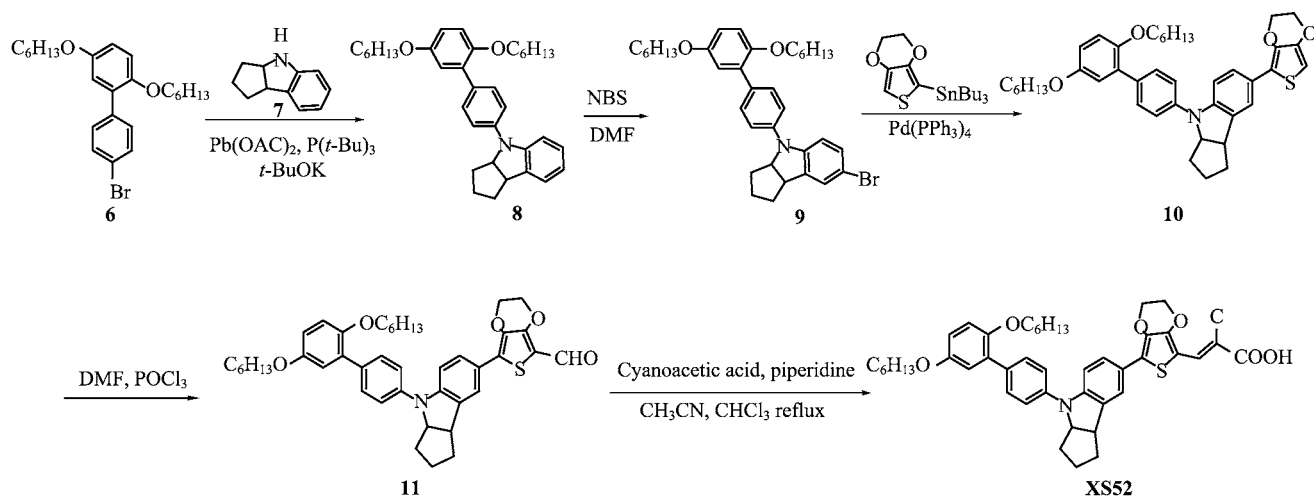
5.9 mmol) and $Pd(PPh_3)_4$ (49 mg, 0.043 mmol) were added into a solution of 15 mL mixture of DME and water (3:1). The mixture was heated to reflux for 6 h. The reaction was quenched by the addition of water (20 mL) and extracted with CH_2Cl_2 (2×20 mL). The combined extracts were dried over anhydrous Na_2SO_4 and filtered. Solvent was removed by rotary evaporation in vacuo to give the crude product, which was purified by column chromatograph packed with silica gel using petroleum ether/ethyl acetate (10:1) as eluent to give a white solid (1.47 g, 70% yield). 1H NMR (400 MHz, $CDCl_3$): δ (ppm) 7.49 (d, $J=8.5$ Hz, 4H), 7.36 (d, $J=8.7$ Hz, 2H), 7.14 (d, $J=8.5$ Hz, 4H), 7.07 (d, $J=8.7$ Hz, 2H), 6.95 (d, $J=2.9$ Hz, 2H), 6.90 (d, $J=8.8$ Hz, 2H), 6.84–6.81 (m, 2H), 3.95 (t, $J=6.5$ Hz, 4H), 3.89 (t, $J=6.4$ Hz, 4H), 1.81–1.77 (m, 4H), 1.73–1.70 (m, 4H), 1.50–1.45 (m, 4H), 1.37–1.36 (m, 12H), 1.31–1.30 (m, 8H), 0.94–0.91 (m, 6H), 0.89–0.88 (m, 6H). ^{13}C NMR (100 MHz, $DMSO-d_6$) $\delta=153.4, 150.2, 146.9, 146.0, 133.3, 132.1, 131.3, 130.4, 125.5, 123.5, 116.9, 114.8, 114.4, 113.7, 71.8, 69.5, 68.6, 59.1, 31.5, 29.4, 25.8, 22.6, 14.1$ ppm.

2. Preparation of compound 4

2-(Tributylstannyl)-3,4-(ethylenedioxy)thiophene (0.52 g, 1.2 mmol), **3** (842 mg, 0.96 mmol), and $Pd(PPh_3)_4$ (60 mg, 0.054 mmol) were dissolved in toluene (20 mL), and the reaction was refluxed under N_2 for 24 h. After cooling down to room temperature, the mixture was poured into water and extracted with CH_2Cl_2 (2×20 mL). The combined organic layers were washed 3 times with water, dried over anhydrous Na_2SO_4 . After rotary evaporation of the solvent under reduced pressure, the residue was purified on a silica



Scheme 1 Synthetic route for XS51.



Scheme 2 Synthetic route for XS52.

gel column (petroleum ether:ethyl acetate=10:1 as eluent) to give a light green oil (325 mg, 35% yield). ^1H NMR (400 MHz, CDCl_3): δ (ppm) 7.64 (d, $J=8.5$ Hz, 2H), 7.51–7.49 (m, 4H), 7.21–7.18 (m, 6H), 6.97 (d, $J=2.9$ Hz, 2H), 6.93 (d, $J=8.8$ Hz, 2H), 6.84–6.83 (m, 2H), 4.33–4.28 (m, 4H), 3.99 (t, $J=6.4$ Hz, 4H), 3.93 (t, $J=6.3$ Hz, 4H), 1.82–1.78 (m, 4H), 1.74–1.71 (m, 4H), 1.49–1.47 (m, 4H), 1.37–1.35 (m, 12H), 1.31–1.30 (m, 8H), 0.93–0.90 (m, 12H). ^{13}C NMR (100 MHz, DMSO-d_6) $\delta=151.2$, 149.9, 147.7, 146.9, 146.1, 133.3, 132.2, 131.3, 130.3, 125.4, 123.2, 116.8, 114.6, 113.9, 112.6, 95.1, 69.2, 65.9, 65.1, 31.5, 29.4, 25.8, 22.7, 14.1 ppm.

3. Preparation of compound 5

To a solution of compound 4 (514 mg, 0.54 mmol) in anhydrous DMF (10 mL, 127 mmol) at 0 °C was added POCl_3 (0.19 mL, 2.1 mmol) dropwise and stirred for 1 h. Subsequently, the mixture was moved into room temperature for another 12 h. The mixture was poured into an ice-water with vigorous stirring, followed by neutralizing with 4 mol/L NaOH. The mixture was extracted with CH_2Cl_2 (3×15 mL), dried over anhydrous Na_2SO_4 . After rotary evaporation of the solvent under reduced pressure, the resulting solid was purified by column chromatography on silica gel (petroleum ether:ethyl acetate=5:1 as eluent) to give a yellow solid (333.8 mg, 64% yield). ^1H NMR (400 MHz,

CDCl₃): δ (ppm) 9.92 (s, 1H), 7.71 (d, $J=8.6$ Hz, 2H), 7.53–7.51 (m, 4H), 7.21–7.17 (m, 6H), 6.96–6.91 (m, 4H), 6.84–6.81 (m, 2H), 4.43–4.39 (m, 4H), 3.98 (t, $J=6.5$ Hz, 4H), 3.93 (t, $J=6.4$ Hz, 4H), 1.81–1.77 (m, 4H), 1.74–1.70 (m, 4H), 1.48–1.46 (m, 4H), 1.36–1.34 (m, 12H), 1.29–1.27 (m, 8H), 0.92–0.91 (m, 12H). ¹³C NMR (100 MHz, DMSO-d₆): $\delta=179.4, 148.6, 148.3, 147.5, 146.2, 138.8, 131.8, 128.8, 128.4, 128.2, 126.4, 124.2, 123.3, 117.0, 115.5, 112.5, 109.5, 67.9, 64.2, 31.0, 28.7, 24.8, 21.8, 12.1$ ppm.

4. Preparation of compound **XS51**

To a mixture of compound **5** (114 mg, 0.12 mmol) and cyanoacetic acid (50 mg, 0.58 mmol) were added acetonitrile (8 mL), chloroform (4 mL) and piperidine (50 μ L). The solution was refluxed for 24 h. After cooling, the solvent was removed in vacuo. The pure product was obtained by silica gel chromatography (CH₂Cl₂:MeOH=10:1 as eluent) as red powder (80.6 mg, 65% yield). Mp>300 °C. IR (KBr): 3428, 2930, 2367, 1632, 1062 cm⁻¹. ¹H NMR (400 MHz, DMSO-d₆): δ (ppm) 8.21 (s, 1H), 7.70 (d, $J=8.8$ Hz, 2H), 7.54–7.52 (m, 4H), 7.13–7.08 (m, 6H), 7.00 (d, $J=8.8$ Hz, 2H), 6.89–6.84 (m, 4H), 4.50–4.42 (m, 4H), 3.94 (t, $J=6.4$ Hz, 4H), 3.89 (t, $J=6.2$ Hz, 4H), 1.71–1.67 (m, 4H), 1.63–1.59 (m, 4H), 1.43–1.39 (m, 4H), 1.31–1.30 (m, 12H), 1.24–1.22 (m, 8H), 0.89–0.80 (m, 12H). ¹³C NMR (100 MHz, DMSO-d₆): $\delta=164.6, 153.3, 150.1, 145.4, 138.0, 134.1, 130.9, 130.7, 128.2, 125.1, 124.4, 122.6, 117.9, 116.5, 115.1, 114.5, 108.7, 69.3, 68.3, 55.3, 31.4, 29.2, 25.6, 22.5, 14.2$ ppm. HRMS (ESI) calculated for C₆₄H₇₆N₂O₈S (M+H⁺): 1033.5400, found 1033.5417.

5. Preparation of compound **8**

To a 100 mL two neck round-bottom flask were added compound **6** (2.00 g, 4.63 mmol), compound **7** (0.88 g, 5.56 mmol), Pd(OAc)₂ (62 mg), *t*-BuOK (624 mg), P(*t*-Bu)₃ (0.6 mL) and toluene (30 mL). The reaction mixture was refluxed overnight under nitrogen. After cooling to room temperature, saturated NH₄Cl was added and extracted with ethyl acetate (3 \times 10 mL). The combined organic layers were washed with brine and then dried over anhydrous magnesium sulfate, filtered, and concentrated in vacuo to give the crude product, which were purified by column chromatograph packed with silica gel using petroleum ether:ethyl acetate (15:1) as eluent to afford a light-yellow solid of compound **8** (1.37 g, 58% yield). Mp: 87–88 °C; IR (KBr): 3454, 2933, 2855, 1597, 1497, 1461, 1384, 1262, 1211, 1051 cm⁻¹; ¹H NMR (400 MHz, CDCl₃): δ (ppm) 7.71 (d, $J=8.6$ Hz, 2H), 7.45 (d, $J=8.6$ Hz, 2H), 7.30–7.18 (m, 3H), 7.10 (d, $J=3.0$ Hz, 1H), 7.02 (d, $J=8.8$ Hz, 1H), 6.92 (dd, $J=8.8$ Hz, $J=3.0$ Hz, 1H), 6.90–6.86 (m, 1H), 4.93–4.88 (m, 1H), 4.08 (t, $J=6.5$ Hz, 2H), 4.01 (t,

$J=6.5$ Hz, 2H), 3.98–3.96 (m, 1H), 2.22–2.12 (m, 2H), 2.05–1.76 (m, 7H), 1.72–1.38 (m, 13H), 1.08–1.01 (m, 6H); ¹³C NMR (100 MHz, CDCl₃): $\delta=153.6, 150.4, 146.9, 142.3, 135.3, 131.8, 131.7, 131.6, 130.3, 127.3, 124.8, 119.4, 118.3, 117.0, 114.6, 114.5, 113.6, 109.2, 69.6, 69.3, 68.7, 45.7, 34.8, 34.0, 31.8, 31.6, 29.6, 29.5, 25.9, 25.9, 24.6, 22.7, 22.7, 14.2, 14.2$ ppm; HRMS (ESI) calculated for C₃₅H₄₆NO₂ (M+H⁺): 512.3450, found: 512.3448.

6. Preparation of compound **9**

To a stirred solution of compound **8** (1.20 g, 2.34 mmol) in DMF (15 mL) was added dropwise a solution of *N*-bromosuccinimide (NBS, 438 mg, 2.46 mmol) dissolved in dimethylformamide (DMF, 5 mL) at room temperature. After the addition, the mixture was stirred overnight in dark. Ice water was added to terminate the reaction and the product was extracted with ethyl acetate. The combined organic layers were washed with brine water and dried with anhydrous MgSO₄. The solvent was evaporated in vacuo. The crude product was purified by column chromatograph packed with silica gel using petroleum ether:ethyl acetate (15:1) as eluent to afford a light-yellow oil of compound **9** (1.36 g, 98% yield). IR (KBr): 3454, 2931, 2852, 1595, 1496, 1390, 1262, 1050 cm⁻¹; ¹H NMR (400 MHz, CDCl₃): δ (ppm) 7.59 (d, $J=8.6$ Hz, 2H), 7.31 (d, $J=8.6$ Hz, 2H), 7.25–7.24 (m, 1H), 7.18 (dd, $J=8.8$ Hz, $J=3.0$ Hz, 1H), 6.97–6.93 (m, 3H), 6.84 (dd, $J=8.8$ Hz, $J=3.0$ Hz, 1H), 4.85–4.81 (m, 1H), 3.99 (t, $J=6.5$ Hz, 2H), 3.92 (t, $J=6.5$ Hz, 2H), 3.89–3.84 (m, 1H), 2.10–2.03 (m, 2H), 1.86–1.68 (m, 7H), 1.54–1.28 (m, 13H), 0.98–0.90 (m, 6H); ¹³C NMR (100 MHz, CDCl₃): $\delta=153.5, 150.3, 146.4, 141.6, 137.5, 131.8, 131.6, 130.3, 129.8, 127.6, 118.4, 117.0, 114.6, 113.6, 109.8, 109.6, 69.6, 69.2, 68.7, 45.4, 34.8, 34.0, 31.6, 31.5, 31.4, 29.7, 29.4, 29.4, 25.8, 25.8, 24.5, 22.6, 22.6, 14.0, 14.0$ ppm; HRMS (ESI) calculated for C₃₅H₄₅BrNO₂ (M+H⁺): 590.2634, found: 590.2632.

7. Preparation of compound **10**

To a 100 mL two-neck round-bottom flask were added Pd(PPh₃)₄ (60 mg), compound **9** (1.15 g, 1.95 mmol), 2-(tributylstannyl)-3,4-(ethelenedioxy)thiophene (1.26 g, 2.92 mmol) and toluene (30 mL) subsequently. The mixture was refluxed overnight under nitrogen. The reaction mixture was quenched by saturated aqueous ammonium chloride solution and extracted with ethyl acetate (3 \times 10 mL). The combined organic layers were washed with brine water and then dried over anhydrous magnesium sulfate, filtered, and concentrated in vacuo to give the crude product, which were purified by column chromatograph packed with silica gel using petroleum ether:ethyl acetate (15:1 to 10:1) as eluent to afford green-yellow oil of compound

10 (660 mg, 52% yield). IR (KBr): 3451, 1729, 1637, 1340, 1287 cm^{-1} ; ^1H NMR (400 MHz, CDCl_3): δ (ppm) 7.52 (d, $J=8.6$ Hz, 2H), 7.30 (d, $J=8.6$ Hz, 2H), 7.23–7.16 (m, 2H), 6.95–6.93 (m, 3H), 6.77 (dd, $J=8.8$ Hz, $J=3.0$ Hz, 1H), 6.25 (s, 1H), 4.90–4.88 (m, 1H), 4.45–4.44 (m, 2H), 4.41–4.40 (m, 2H), 3.99 (t, $J=6.60$ Hz, 2H), 3.95–3.90 (m, 3H), 2.15–2.07 (m, 2H), 1.94–1.76 (m, 7H), 1.45–1.30 (m, 13H), 0.98–0.90 (m, 6H); ^{13}C NMR (100 MHz, CDCl_3): $\delta=167.7, 167.7, 148.2, 143.4, 132.3, 132.3, 130.9, 130.9, 128.8, 128.6, 121.3, 120.1, 117.5, 113.4, 109.8, 109.5, 65.6, 65.5, 42.3, 34.5, 33.8, 31.6, 30.6, 29.7, 29.4, 29.3, 25.8, 22.6, 19.2, 19.0, 14.0, 13.7, 13.7$ ppm; HRMS (ESI) calculated for $\text{C}_{41}\text{H}_{50}\text{NO}_4\text{S}$ ($\text{M}+\text{H}^+$): 652.3461, found: 652.3459.

8. Preparation of compound **11**

POCl_3 (412 mg, 2.69 mmol) was added dropwise to dry DMF (7 mL) at 0°C . The reaction was stirred at 0°C for 30 min and a solution of compound **10** (350 mg, 0.54 mmol) in dry DMF (5 mL) was added via a syringe. After the addition, the mixture was stirred for 4 h at room temperature. Ice water was added to terminate the reaction, and the product was extracted with ethyl acetate (3×10 mL). The combined organic layers were washed with brine and then dried over anhydrous magnesium sulfate, filtered, and concentrated in vacuo. The crude product was purified by column chromatograph packed with silica gel using petroleum ether:ethyl acetate (10:1 to 5:1) to give a yellow solid of aldehyde **11** (297 mg, 81% yield). Mp: $109\text{--}110^\circ\text{C}$; IR (KBr): 3454, 2926, 2360, 1646, 1445, 1400, 1084 cm^{-1} ; ^1H NMR (400 MHz, CDCl_3): δ (ppm) 9.90 (s, 1H), 7.60–7.55 (m, 4H), 7.33 (d, $J=8.6$ Hz, 2H), 7.06 (d, $J=8.8$ Hz, 1H), 6.96 (d, $J=3.0$ Hz, 1H), 6.93 (d, $J=9.0$ Hz, 1H), 6.83 (dd, $J=8.8$ Hz, $J=3.0$ Hz, 1H), 4.92–4.89 (m, 1H), 4.43–4.42 (m, 2H), 4.40–4.39 (m, 2H), 3.98 (t, $J=6.6$ Hz, 2H), 3.93–3.88 (m, 3H), 2.14–2.00 (m, 2H), 1.90–1.69 (m, 7H), 1.43–1.28 (m, 13H), 0.96–0.89 (m, 6H); ^{13}C NMR (100 MHz, CDCl_3): $\delta=179.0, 153.5, 150.3, 149.2, 148.2, 141.0, 136.1, 135.7, 132.3, 131.6, 131.2, 130.3, 127.0, 123.4, 122.2, 119.1, 117.0, 114.6, 113.8, 113.7, 107.9, 69.6, 69.2, 68.7, 65.2, 64.5, 53.4, 45.3, 35.0, 33.8, 31.6, 31.5, 29.4, 29.4, 26.9, 25.8, 25.8, 24.4, 22.6, 22.6, 14.0$ ppm; HRMS (ESI) calculated for $\text{C}_{42}\text{H}_{50}\text{NO}_5\text{S}$ ($\text{M}+\text{H}^+$): 680.3461, found: 680.3459.

9. Preparation of compound **XS52**

To a stirred solution of compound **11** (270 mg, 0.4 mmol) and cyanoacetic acid (52 mg, 0.6 mmol) in acetonitrile (10 mL) were added chloroform (6 mL) and piperidine (120 μL , 1.2 mmol). The reaction mixture was refluxed for 8 h. Additional cyanoacetic acid (34 mg, 0.4 mmol) and piperidine (80 μL , 0.8 mmol) were added. The mixture was refluxed for additional

8 h and then acidified with 1 mol/L hydrochloric acid aqueous solution (10 mL). The crude product was extracted with CH_2Cl_2 (3×10 mL). The combined organic layers were washed with brine and then dried over anhydrous magnesium sulfate, filtered, and concentrated in vacuo to give the crude product. The residue was purified by column chromatography packed with silica gel using $\text{CH}_2\text{Cl}_2/\text{CH}_3\text{OH}$ (20:1 to 10:1) as eluent to give red powder of **XS52** (281 mg, 94% yield). Mp: $176\text{--}178^\circ\text{C}$; IR (KBr): 3453, 1636, 1518, 1403, 1249 cm^{-1} ; ^1H NMR (400 MHz, DMSO-d_6): δ ppm 8.18 (s, 1H), 7.58–7.54 (m, 4H), 7.35 (d, $J=8.6$ Hz, 2H), 7.04 (d, $J=8.8$ Hz, 1H), 7.00 (d, $J=9.0$ Hz, 1H), 6.88 (d, $J=3.0$ Hz, 1H), 6.84 (dd, $J=8.8$ Hz, $J=3.0$ Hz, 1H), 5.02–4.94 (m, 1H), 4.51–4.49 (m, 2H), 4.45–4.40 (m, 2H), 4.00 (t, $J=6.85$ Hz, 2H), 3.90–3.87 (m, 3H), 1.73–1.58 (m, 6H), 1.37–1.23 (m, 16H), 0.88–0.83 (m, 6H); ^{13}C NMR (100 MHz, CDCl_3): $\delta=153.4, 150.3, 150.0, 148.8, 142.2, 140.6, 136.2, 135.9, 133.7, 132.7, 131.4, 130.4, 127.8, 123.7, 121.9, 119.4, 117.3, 117.0, 114.5, 113.7, 108.8, 107.7, 69.6, 69.2, 68.7, 65.5, 64.4, 45.1, 35.2, 33.6, 31.9, 31.6, 31.5, 30.3, 29.7, 29.4, 29.3, 25.8, 25.8, 24.4, 22.6, 22.6, 14.0, 14.0$ ppm; HRMS (ESI) calculated for $\text{C}_{45}\text{H}_{51}\text{N}_2\text{O}_6\text{S}$ ($\text{M}+\text{H}^+$): 747.3468, found: 747.3466.

C. Optical and electrochemical measurements

The absorption spectra of the dyes were measured by HITACHI U-3310 spectrophotometer. Fluorescence measurements were carried out with a HITACHI F-4500 fluorescence spectrophotometer. Cyclic voltammetry (CV) measurements for the dye-sensitized films were performed on a Zennium electrochemical workstation (ZAHNER), with sensitized electrodes as working electrode, Pt-wires as counter electrode, and an Ag/AgCl electrode as reference electrode with a scan rate of 50 mV/s. Tetrabutylammonium perchlorate (TBAP, 0.1 mol/L) and MeCN were used as supporting electrolyte and solvent, respectively. The measurements were calibrated with ferrocene as standard.

Charge densities at open circuit and intensity modulated photovoltage spectroscopy (IMVS) were performed on Zennium electrochemical workstation (ZAHNER, Germany), which includes a green light-emitting diode (LED, 532 nm) and the corresponding control system. The intensity-modulated spectra were measured at room temperature with light intensity ranging from 5 W/m^2 to 75 W/m^2 , modulation frequency ranging from 0.1 Hz to 10 kHz, and modulation amplitude less than 5% of the light intensity.

D. Fabrication and characterization of DSCs

The TiO_2 paste (particle size, 20 nm) was printed on a conducting glass (Nippon Sheet Glass, Hyogo, Japan, fluorine-doped SnO_2 over layer, sheet resistance

of 10 Ω/sq) using a screen printing technique. The film was dried in air at 120 $^{\circ}\text{C}$ for 30 min and calcined at 500 $^{\circ}\text{C}$ for 30 min under flowing oxygen before cooling to room temperature. The heated electrodes were impregnated with a 0.05 mol/L titanium tetrachloride solution in a water-saturated desiccator at 70 $^{\circ}\text{C}$ for 30 min and fired again to give a ca. 3 μm thick mesoscopic TiO_2 film. The TiO_2 electrode was stained by immersing it into a 0.5 mmol/L dye solution in a mixture of DCM/EtOH (volume ratio, 1:1) and kept at room temperature for 16 h to complete the sensitizer uptake. Then the sensitized electrodes were rinsed with dry ethanol and dried by a dry air flow. Pt catalyst was deposited on the FTO glass by coating with a drop of H_2PtCl_6 solution (40 mmol/L in ethanol) with the heat treatment at 395 $^{\circ}\text{C}$ for 15 min to give photoanode. The sensitized electrode and Pt-counter electrode were assembled into a sandwich type cell by a 25 μm -thick Surlyn (DuPont) hot-melt gasket and sealed up by heating. The DSCs had an active area of 0.16 cm^2 and electrolyte composed of 0.25 mol/L $[\text{Co}(\text{II})(\text{phen})_3](\text{PF}_6)_2$, 0.05 mol/L $[\text{Co}(\text{III})(\text{phen})_3](\text{PF}_6)_3$, 0.5 mol/L 4-terpyridine (TBP) and 0.1 mol/L lithium bis-(trifluoromethanesulfonyl)imide (LiTFSI) in acetonitrile. For comparison, the iodine electrolyte composed of 0.6 mol/L 1,2-dimethyl-3-n-propylimidazolium iodide (DMPII), 0.1 mol/L LiI , 0.05 mol/L I_2 , and 0.5 mol/L tertbutylpyridine in acetonitrile was tested as well.

The photocurrent-voltage (J - V) characteristics of the solar cells were carried out with Keithley 2400 digital source meter controlled by a computer and a standard AM1.5 solar simulator-Oriel 91160-1000 (300 W) SOLAR SIMULATOR 2 \times 2 BEAM. The light intensity was calibrated by an Oriel reference solar cell. A metal mask with an aperture area of 0.2 cm^2 was covered on a testing cell during all measurements. The action spectra of monochromatic incident photon-to-current conversion efficiency (IPCE) for solar cells were performed by a commercial setup (QTest Station 2000 IPCE Measurement System, CROWNTech, USA).

III. RESULTS AND DISCUSSION

A. UV-Vis absorption and electrochemical properties

The UV-Vis absorption spectra of dyes **XS51** and **XS52** are shown in Fig.2, and the photophysical properties are summarized in Table I. Both of the dyes have a relatively broad and strong absorption in the ultraviolet and visible region, and exhibit intramolecular charge-transfer transition (ICT) electron transition peaks located in the range of 400–600 nm. The major absorption peaks for **XS51** and **XS52** locate at 512 and 536 nm, respectively. In comparison with **XS51**, **XS52** shows a red-shifted absorption due to the powerful electron-donating capability of the indoline unit.

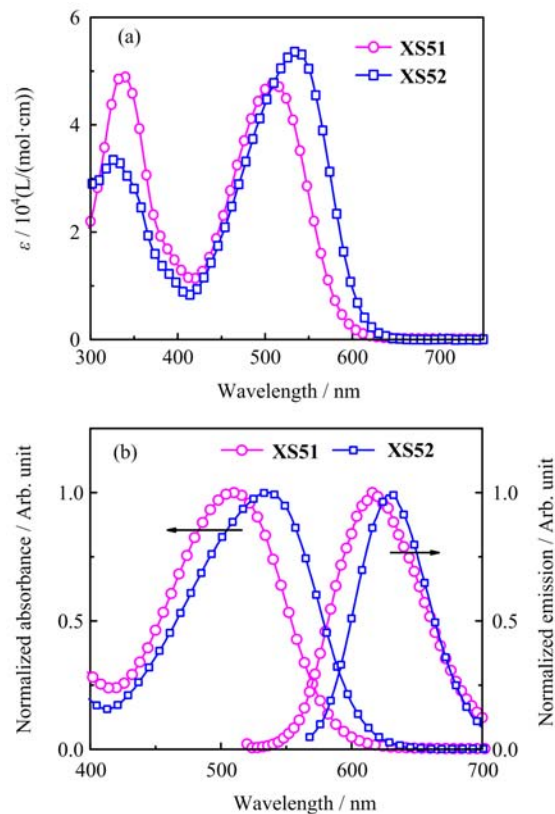


FIG. 2 (a) UV-Vis absorption spectra of **XS51** and **XS52** in dichloromethane. (b) Normalized absorption and emission spectra of **XS51** and **XS52**.

TABLE I Optical properties and electrochemical properties of the dyes (λ in nm, ϵ in $\text{L}/(\text{mol}\cdot\text{cm})$, E_{0-0} in eV, and E_{ox} and E_{ox^*} in V).

Dye	$\lambda_{\text{max}}^{\text{a}}$ (ϵ) ^a	$\lambda_{\text{max}}^{\text{b}}$	$\lambda_{\text{int}}^{\text{c}}$	E_{0-0}^{d}	E_{ox}^{e}	$E_{\text{ox}^*}^{\text{f}}$
XS51	512 (4.8×10^4)	615	570	2.18	0.96	-1.22
XS52	536 (5.3×10^4)	629	590	2.10	0.78	-1.32

^a Absorption and ^b emission peaks of dyes measured in CH_2Cl_2 , ϵ is the extinction coefficient at λ_{max} of absorption.

^c The intersect of the normalized absorption and the emission spectra.

^d E_{0-0} values were estimated from the intersections of normalized absorption and emission spectra (λ_{int}): $E_{0-0} = 1240/\lambda_{\text{int}}$.

^e E_{ox} was recorded by cyclic voltammograms of the dye-loaded TiO_2 film.

^f E_{ox^*} was calculated from $E_{\text{ox}} - E_{0-0}$.

The values of molar extinction coefficient, ϵ , at the maximum absorption wavelength for **XS51** and **XS52** are 4.8×10^4 and 5.3×10^4 $\text{L}/(\text{mol}\cdot\text{cm})$, respectively. The high absorption coefficient indicates a good ability of light harvesting, which is desirable for a thin TiO_2 film. When the two dyes are excited by visible light, they exhibit strong luminescence maxima at 550 nm to 700 nm

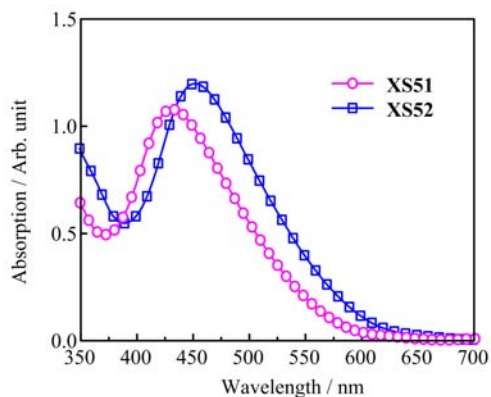


FIG. 3 Absorption spectra of sensitized electrodes with **XS51** and **XS52**.

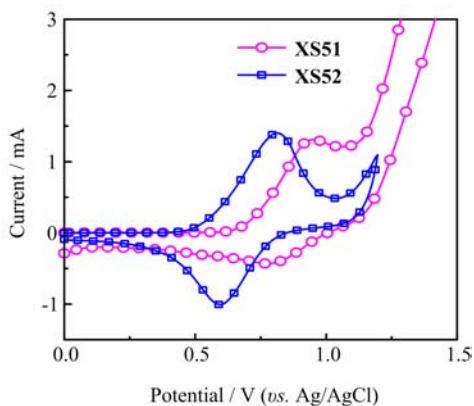


FIG. 4 Cyclic voltammograms of the **XS51**- and **XS52**-loaded TiO_2 films.

(Fig.2(b)).

The absorption spectra of **XS51** and **XS52** anchored on transparent mesoporous titania films (3 μm) are shown in Fig.3. The absorption maximum of **XS51** lies at 432 nm, for **XS52** at 452 nm. In contrast to their absorption peaks in solution, both of them show hypsochromic shifts, which could be ascribed to a weaker electron-withdrawing capability of the carboxylate titanium assembly than that of carboxylic acid [22].

Electrochemical properties of **XS51** and **XS52** are presented in Table I. The redox potentials of dyes are obtained by cyclic voltammetric (CV) curve with 0.1 mol/L tetrabutylammonium hexafluorophosphate in acetonitrile solution, and representative cyclic voltammograms are shown in Fig.4. The first quasi-reversible one-electron oxidation wave is taken as the ground-state oxidation potentials (E_{ox}). The E_{ox} values of **XS51** and **XS52** are calculated to be 0.96 and 0.78 V (*vs.* NHE), respectively, which are more positive than the $[\text{Co}(\text{II}/\text{III})(1,10\text{-phenanthroline})_3]^{n+}$ redox couple (0.62 V *vs.* NHE) [23]. It can be said that the driving force from the cobalt to the dyes is sufficient and the oxidized dyes will favorably accept electrons from Co(II) ions to be regenerated.

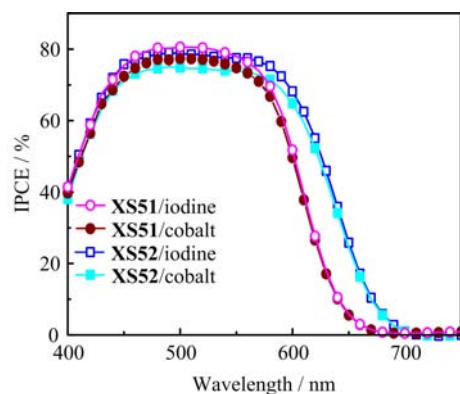


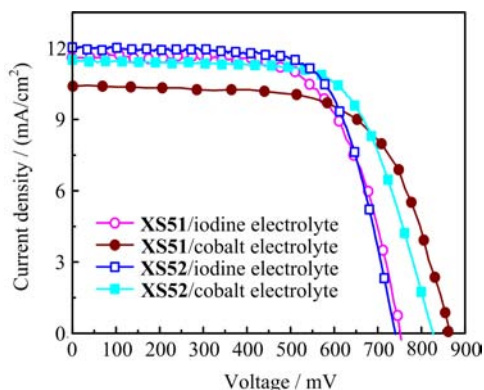
FIG. 5 Incident photon-to-current conversion efficiency spectra of DSCs.

The excited-state reduction potential (E_{ox^*}) of the dyes are calculated from the ground-state oxidation potentials (E_{ox}) and the 0-0 band gaps (E_{0-0}), which is determined from the intersection of absorption and emission spectra. The E_{ox^*} values of **XS51** and **XS52** are calculated to be -1.22 and -1.32 V *vs.* NHE, respectively. The more negative value of **XS52** is originated from the stronger electron-donating capability of indoline unit than that of triarylamine. Both are much more negative than the conduction band of TiO_2 at approximate -0.5 V *vs.* NHE. Therefore, these dyes used as sensitizers will produce sufficient driving forces for electron injection from the excited dye molecules to the conduction band of TiO_2 electrode.

B. Photovoltaic performance of DSCs

The incident monochromatic photon-to-current conversion efficiency (IPCE) was obtained with a sandwich cell employing cobalt and iodine electrolytes, respectively. IPCE spectra based on **XS51** and **XS52** can be seen from Fig.5. Both of the dyes show higher IPCE values in iodine electrolytes than in cobalt electrolytes. For example, the top IPCE value of **XS51** is 80.6% for iodine electrolyte and 78.7% for cobalt electrolyte. A little lower IPCE values of **XS52** were observed in iodine and cobalt electrolyte corresponding to those of **XS51**. However, **XS52** shows obviously broader IPCE spectra than **XS51**, which is in accordance with the preceding light absorption measurements. The broad IPCE spectrum is beneficial to high photocurrent density of DSCs.

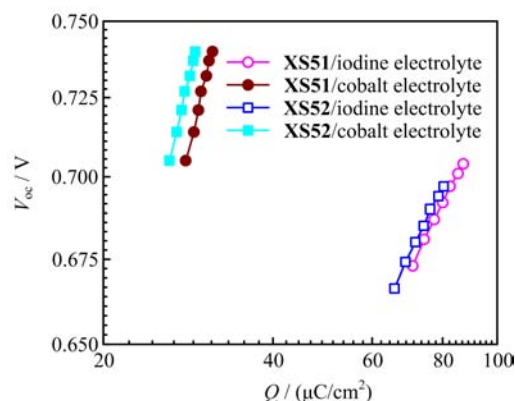
J - V curves of the devices based on **XS51** and **XS52** in electrolytes of $[\text{Co}(\text{II})(\text{phen})_3](\text{PF}_6)_2$ are measured under AM 1.5 irradiation (100 mW/cm^2), and the results are shown in Fig.6. The detailed photovoltaic parameters are summarized in Table II. A relatively thin titania film (3 μm) was applied so as to minimize the mass transport limitation of $\text{Co}(\text{II}/\text{III})(\text{phen})_3$ redox couple. As it can be seen from Table II, 5.88% of so-

FIG. 6 J - V characteristics of DSCs.TABLE II Photovoltaic performance of DSCs employing cobalt or iodine electrolytes (J_{sc} in mA/cm^2).

Dye	Electrolyte	J_{sc}	V_{oc}/mV	FF	PCE/%
XS51	EL-cobalt	10.5	862	0.65	5.88
	EL-iodide	11.6	751	0.67	5.68
XS52	EL-cobalt	11.5	830	0.68	6.58
	EL-iodide	12.0	740	0.69	6.13

lar energy to power conversion efficiency (PCE) based on **XS51** is achieved with a J_{sc} of $10.5 \text{ mA}/\text{cm}^2$, a V_{oc} of 860 mV , and a fill factor (FF) of 0.65 . The cells based on **XS52** show an increased J_{sc} of $11.5 \text{ mA}/\text{cm}^2$ and a decreased V_{oc} of 830 mV . The improvement of J_{sc} compensates for a slight drop in V_{oc} , contributing to an enhanced PCE of 6.58% . The observed results here suggest that indoline donor with strong electron-donating capability induce the improvements of J_{sc} in comparison with triaryamine donor, which is in agreement with the observed light absorption and IPCEs. The increased V_{oc} obtained for **XS51** can be attributed to the sterically bulky four hexyloxy groups on the dye, which prevent Co(III) ions at the vicinity of the TiO_2 from recombining at the titania/electrolyte interface.

We have also recorded the J - V curves of the DSCs employing an iodine electrolyte consisting of 0.25 mol/L DMPImI, 0.1 mol/L LiTFSI, 0.05 mol/L I_2 , and 0.5 mol/L TBP in acetonitrile for comparison, and the detailed photovoltaic parameters are listed in Table II. A similar trend in J_{sc} and V_{oc} can be found for the two dyes. The cells based on **XS52** employing iodine electrolyte show higher J_{sc} and enhanced FF, corresponding to an improved PCE in contrast to those of the cells based on **XS51**. On the other hand, for the same dye, the cobalt electrolyte DSCs evidently outperform the devices based on the conventional iodide/triiodide redox couple. For example, the cell based on **XS52** with cobalt electrolyte generates an improved V_{oc} (830 mV *vs.* 740 mV) in comparison with the iodine electrolyte, resulting in an enhanced PCE. The efficiency gain is pri-

FIG. 7 Dependence of open circuit V_{oc} on charge density Q for DSCs.

marily due to the significant increase in V_{oc} , which compensates for a minor drop in J_{sc} . These results indicate that the synthesized **XS51** and **XS52** are more suitable for Co(II/III) tris(phen) redox couple than I^-/I_3^- redox couple in assembling DSCs.

C. Dependence of photovoltage on the conduction band movement and charge recombination

The respectable increase of V_{oc} obtained by the delicate change in molecular structure is intriguing. To scrutinize the origin of the improvement in V_{oc} , we discuss the influence factors on the photovoltage. Generally, V_{oc} of a DSC is dependent on the difference between the Fermi-level of TiO_2 ($E_{F,n}$) and redox electrolyte ($E_{F,\text{redox}}$), *i.e.* $V_{oc} = E_{F,\text{redox}} - E_{F,n}$ [24]. As for a fixed redox electrolyte, $E_{F,\text{redox}}$ will not change obviously in DSCs. $E_{F,n}$ of TiO_2 can be expressed as

$$E_{F,n} = E_{CB} + k_B T \ln \frac{n_c}{N_c} \quad (1)$$

where E_{CB} is the conduction band of TiO_2 , k_B is the Boltzmann constant, T is the temperature (293 K in this work), n_c is the free electron density on TiO_2 and N_c is the density of accessible states in the conduction band of TiO_2 [25]. As shown in Eq.(1), $E_{F,n}$ depends on the variation of E_{CB} and n_c . Correspondingly, when $E_{F,\text{redox}}$ is fixed, V_{oc} is intimately correlated to E_{CB} and n_c . The relative conduction band positions and electron lifetimes of DSCs based on **XS51** and **XS52** were investigated to clarify the variation of V_{oc} in performance of cells.

Charge densities and electron lifetimes (τ_{oc}) at open-circuit were measured by charge extraction technique and by controlled intensity modulated photovoltage spectroscopy (IMVS), respectively. Figure 7 shows the relationship between V_{oc} and the extracted charge density (Q) at open circuit. The curves for the DSCs based on **XS51** and **XS52** are roughly parallel to each other. At a fixed Q , **XS52** cells, both with cobalt and iodine

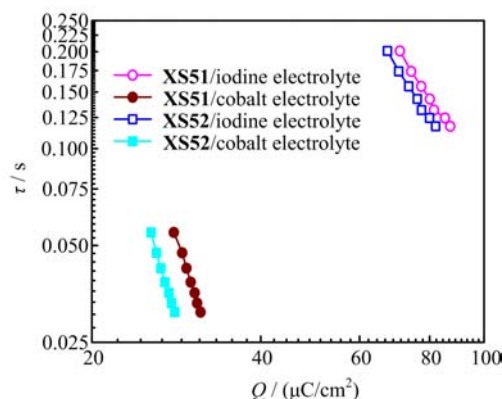


FIG. 8 Dependence of electron lifetime τ on charge density Q .

electrolytes, show higher V_{oc} than their counterparts, which means that indoline moiety is preferable to triarylamine unit because it can lead more negative shift of the conduction band edge position of TiO_2 . As seen in Eq.(1), a more negative shift of E_{CB} will provide a possibility of V_{oc} improvement.

Figure 8 shows the dependence of electron lifetime on charge density at open circuit. Typical data are illustrated in Table III. At the same Q , the electron lifetime of **XS51** based DSCs is much longer than that of **XS52**, indicating that charge recombination between electrons in TiO_2 film and Co(III) ions in the electrolyte are significantly retarded by the four hexyloxyl groups on triarylamine moiety. Since the different shift of E_{CB} is observed in Fig.7, **XS52** based DSCs might provide higher V_{oc} than those of **XS51**. On the other hand, **XS51** based DSCs show longer electron lifetime than those of **XS52**. In combination with E_{CB} and electron lifetime, the improvement in V_{oc} is mainly ascribed to the retarded charge recombination rather than the different positions of the conduction band edge of TiO_2 . These results indicate that indoline dye is beneficial to more negative shift of E_{CB} , but the bulky substituent on the dye is not enough for retardation of interfacial charge recombination in DSCs. The triarylamine dye with four hexyloxyl groups shows an improvement of photovoltage through full steric hindrance, which prevents back-recombination and prolongs the electron lifetime in the semiconductor.

IV. CONCLUSION

We have developed two new dyes **XS51** and **XS52** based on triarylamine and indoline, respectively, for dye-sensitized solar cells (DSCs). The indoline dye **XS52** shows a red-shifted absorption and higher molar extinction coefficient than the triarylamine dye. High short-circuit photocurrent density is obtained for **XS52** due to the strong electron-donating capability of indoline unit. The two hexyloxyl groups on indoline dye

TABLE III Electron lifetime data under different charge densities (Q in $\mu C/cm^2$).

Q	τ/s (EL-iodine)		Q	τ/s (EL-cobalt)	
	XS51	XS52		XS51	XS52
70	0.201	0.174	25.5		0.055
73		0.156	26.5		0.043
74	0.174		28	0.055	0.031
77	0.156		30	0.038	
80	0.143	0.125	31.2	0.031	

are not enough for retardation of charge recombination at the titania/electrolyte interface in DSCs, which leads to a little lower open-circuit voltage in comparison with **XS51**. The photovoltaic performances of the Co(II/III)tris(phen) redox couple are superior to those of I^-/I_3^- redox couple for thin-film DSCs sensitized by **XS51-XS52**, indicating that rational design of sterically bulky organic dyes is needed for further development of high-efficiency iodine-free devices.

V. ACKNOWLEDGMENTS

This work was supported by the National Natural Science Foundation of China (No.21376179, No.21103123) and the Massive Open Online Courses Project in Tianjin University of Technology.

- [1] A. Yella, H. W. Lee, H. N. Tsao, C. Yi, A. K. Chandiran, M. K. Nazeeruddin, E. W. G. Diau, C. Y. Yeh, S. M. Zakeeruddin, and M. Grätzel, *Science* **334**, 629 (2011).
- [2] A. Hagfeldt, G. Boschloo, L.C. Sun, L. Kloo, and H. Pettersson, *Chem. Rev.* **110**, 6595 (2010).
- [3] M. Liang and J. Chen, *Chem. Soc. Rev.* **42**, 3453 (2013).
- [4] G. Boschloo and A. Hagfeldt, *Acc. Chem. Res.* **42**, 1819 (2009).
- [5] B. C. O'Regan, I. López-Duarte, M. V. Martínez-Díaz, A. Forneli, J. Albero, A. Morandeira, E. Palomares, T. Torres, and J. R. Durrant, *J. Am. Chem. Soc.* **130**, 2906 (2008).
- [6] T. Marinado, K. Nonomura, J. Nissfolk, M. K. Karlsson, D. P. Hagberg, L. C. Sun, S. Mori, and A. Hagfeldt, *Langmuir* **26**, 2592 (2010).
- [7] M. Planells, L. Pelleja, J. N. Clifford, M. Pastore, D. Angelis, F. López, N. Marder, and S. R. Palomares, *Energy Environ. Sci.* **4**, 1820 (2011).
- [8] A. Hagfeldt and M. Grätzel, *Chem. Rev.* **95**, 49 (1995).
- [9] H. Nusbauer, S. M. Zakeeruddin, J. E. Moser, and M. Grätzel, *Chem. Eur. J.* **9**, 3756 (2003).
- [10] S. M. Feldt, E. A. Gibson, E. Gabriellson, L. C. Sun, G. Boschloo, and A. Hagfeldt, *J. Am. Chem. Soc.* **132**, 16714 (2010).

- [11] S. M. Feldt, G. Wang, G. Boschloo, and A. Hagfeldt, *J. Phys. Chem. C* **115**, 21500 (2011).
- [12] H. N. Tian and L. C. Sun, *J. Mater. Chem.* **21**, 10592 (2011).
- [13] B. C. O'Regan and M. Grätzel, *Nature* **353**, 737 (1991).
- [14] U. Bach, D. Lupo, P. Comte, J. E. Moser, F. Weissörtel, J. Salbeck, H. Spreitzer, and M. Grätzel, *Nature* **395**, 583 (1998).
- [15] M. M. Lee, J. Teuscher, T. Miyasaka, T. N. Murakami, and H. J. Snaith, *Science* **338**, 643 (2012).
- [16] J. H. Yum, E. Baranoff, F. Kessler, T. Moehl, S. Ahmad, T. Bessho, A. Marchioro, E. Ghadiri, J. E. Moser, C. Yi, M. K. Nazeeruddin, and M. Grätzel, *Nat. Commun.* **3**, 631 (2012).
- [17] Y. Bai, J. Zhang, D. Zhou, Y. Wang, M. Zhang, and P. Wang, *J. Am. Chem. Soc.* **133**, 11442 (2011).
- [18] H. Nusbaumer, J. E. Moser, S. M. Zakeeruddin, M. K. Nazeeruddin, and M. Grätzel, *J. Phys. Chem. B* **105**, 10461 (2001).
- [19] H. X. Wang, P. G. Nicholson, L. Peter, S. M. Zakeeruddin, and M. Grätzel, *J. Phys. Chem. C* **114**, 14300 (2010).
- [20] Y. Liu, J. R. Jennings, Y. Huang, Q. Wang, S. M. Zakeeruddin, and M. Grätzel, *J. Phys. Chem. C* **115**, 18847 (2011).
- [21] G. Li, M. Liang, Z. Sun, H. Wang, L. N. Wang, Z. Wang, and S. Xue, *Chem. Mater.* **25**, 1713 (2013).
- [22] D. Zhou, N. Cai, H. Long, M. Zhang, Y. Wang, and P. Wang, *J. Phys. Chem. C* **115**, 3163 (2011).
- [23] A. Yella, R. Humphry-Baker, B. Curchod, N. Astani, J. Teuscher, and L. Polander, *Chem. Mater.* **25**, 2733 (2013).
- [24] A. Usami, S. Seki, Y. Mita, H. Kobayashi, H. Miyashiro, and N. Terada, *Sol. Energy Mater. Sol. Cells* **93**, 840 (2009).
- [25] D. Zhou, Q. Yu, N. Cai, Y. Bai, Y. Wang, and P. Wang, *Energy Environ. Sci.* **4**, 2030 (2011).